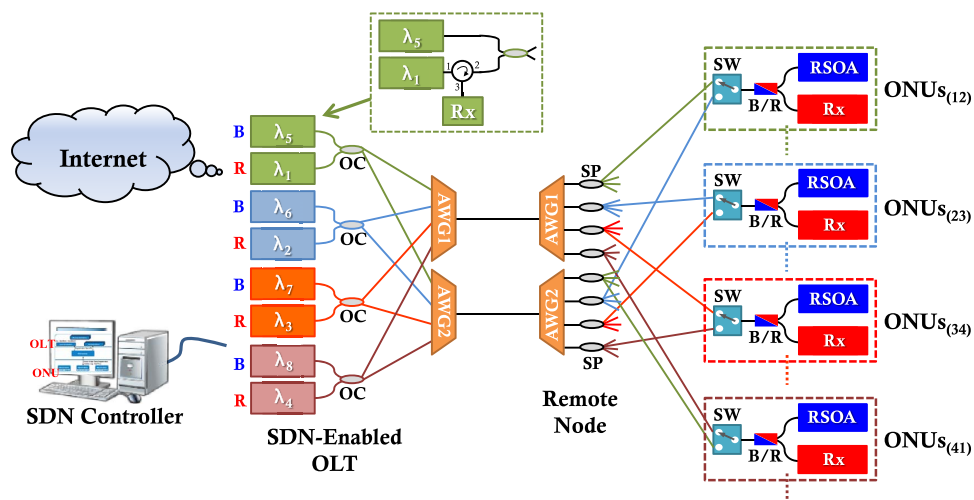


A Flexible and Reliable 40-Gb/s OFDM Downstream TWDM-PON Architecture

Volume 7, Number 6, December 2015

Chien-Hung Yeh
 Chi-Wai Chow
 Ming-Hsiao Yang
 Dar-Zu Hsu



DOI: 10.1109/JPHOT.2015.2504970
 1943-0655 © 2015 IEEE

A Flexible and Reliable 40-Gb/s OFDM Downstream TWDM-PON Architecture

Chien-Hung Yeh,¹ Chi-Wai Chow,² Ming-Hsiao Yang,³ and Dar-Zu Hsu³

¹Department of Photonics, Feng Chia University, Taichung 40724, Taiwan

²Department of Photonics and Institute of Electro-Optical Engineering,
National Chiao Tung University, Hsinchu 30010, Taiwan

³Information and Communications Research Laboratories, Industrial Technology
Research Institute, Hsinchu 31040, Taiwan

DOI: 10.1109/JPHOT.2015.2504970

1943-0655 © 2015 IEEE. Translations and content mining are permitted for academic research only.

Personal use is also permitted, but republication/redistribution requires IEEE permission.

See http://www.ieee.org/publications_standards/publications/rights/index.html for more information.

Manuscript received October 19, 2015; revised November 24, 2015; accepted November 25, 2015. Date of publication December 4, 2015; date of current version December 11, 2015. This paper was supported in part by the Ministry of Science and Technology of Taiwan under Grant MOST-103-2218-E-035-011-MY3, Grant MOST-103-2221-E-009-030-MY3, and Grant MOST-104-2628-E-009-011-MY3; by Aim for the Top University Plan; and by the Ministry of Education. Corresponding author: C.-H. Yeh (e-mail: yehch@fcu.edu.tw).

Abstract: In this paper, a flexible and reliable 40-Gb/s time and wavelength division multiplexing passive optical network (TWDM-PON) architecture is proposed and demonstrated. Here, a 4×10 Gb/s orthogonal frequency-division multiplexing (OFDM) downstream signal is achieved by utilizing four 2.5-GHz directly modulated lasers in the optical line terminal. A reflective optical semiconductor amplifier is utilized in each optical network unit to serve as upstream transmitter (Tx) transmitting 2.5-Gb/s on-off keying (OOK) and 10-Gb/s OFDM upstream traffic, respectively. In addition, the dynamic bandwidth (capacity) allocation and fiber fault protection also can be achieved by applying the new proposed PON architecture with software-defined networking approach.

Index Terms: Time and wavelength division multiplexing (TWDM), passive optical network (PON), software-defined networking (SDN).

1. Introduction

Owing to the popularity of various broadband access applications, an enormous increase in bandwidth requirement has been achieved in recent years. The conventional 2.5 Gbit/s to 10 Gbit/s time division multiplexing passive optical networks (TDM-PONs) could not meet these broadband requirements [1], [2]. Therefore, various organizations have suggested different network architectures to meet the bandwidth request. The Full Service Access Network (FSAN) has finished the potential future-proof access solutions. It has separated the PON evolution into two stages. The first stage is the next-generation PON (NG-PON1), which contains the XG-PON providing the 10 Gbit/s downstream and 2.5 Gbit/s upstream data rates, respectively [3]. The second stage is the NG-PON2, which is expected to deliver the 40 Gbit/s downstream and 10 Gbit/s upstream. For the NG-PON2, many operators have studied different access solutions [4]. These proposed methods include utilizing serial 40G TDM-PON [5], employing orthogonal frequency division multiplexing (OFDM)-PON [6]–[8], and using time and wavelength division multiplexing (TWDM)-PON [9]–[11]. Among these proposed access systems, TWDM-PON can offer a range of bit rates to end-users (2.5–10 Gbps), support symmetrical or asymmetrical bandwidth, and assign different bandwidths to different

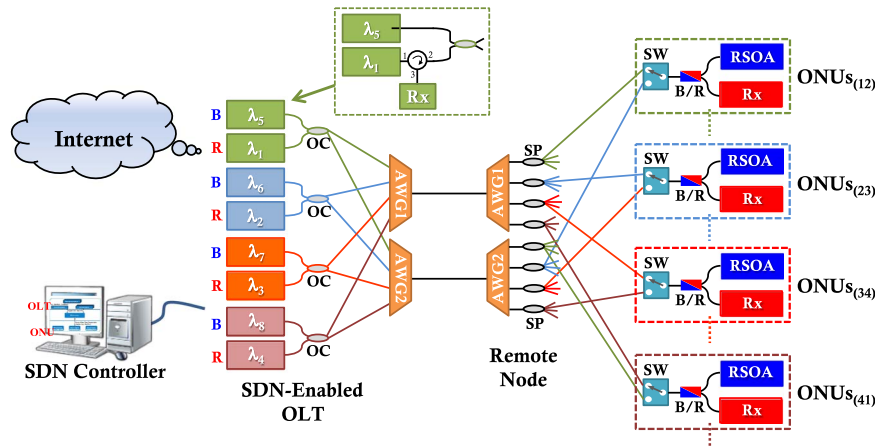


Fig. 1. Proposed 40 Gbit/s OFDM downstream TWDM-PON architecture.

wavelengths. Hence, TWDM-PON would be considered as a main access network for NG-PON2. Moreover, TWDM-PON could reuse the existing optical network unit (ONU) with less destruction and capital investment [9]. Recently, advanced TWDM-PON has been proposed and demonstrated [12]. However, these proposed TWDM-PON systems require the optical tunable transmitters (Tx) and tunable receivers (Rx) in the ONUs for signal traffic. It would result in a higher cost for TWDM-PON access.

Furthermore, TWDM-PON must also offer the high quality of service and reliability to end-user. When fibers between the optical line terminal (OLT) and ONUs are broken in PON architecture, the signal traffic cannot reach the affected ONU and lead to data loss [13]. Therefore, the self-protection management of fiber-fault is one of the essential points in PON system [14]–[16]. To increase the spectral efficiency and reduce the cost of high speed transmitters (Tx) and receivers (Rx), optical orthogonal frequency division multiplexing-quadrature amplitude modulation (OFDM-QAM) signal has been proposed and investigated [17], [18]. Hence the optical OFDM modulation would be a hopeful candidate for the new generation TWDM-PON. In addition, the software defined networking (SDN) technology can enable cloud architectures by delivering automated, on-demand application delivery and mobility [19]. SDN enhances the benefits of data center virtualization, increasing resource flexibility and utilization; and reducing infrastructure costs and overhead [20]. Recently, using the SDN management to improve and enhance the data traffic of PON access has also been proposed and investigated [21].

In this paper, we propose and demonstrate a flexible and reliable 40 Gbit/s OFDM TWDM-PON access architecture. Here, 4×10 Gbit/s OFDM downstream traffic is achieved by using four 2.5 GHz directly modulated lasers (DMLs) in the OLT. Besides, we also use four CW carrier distributed wavelengths as seeding light sources in the OLT for upstream modulation. Reflective optical semiconductor amplifier (RSOA) is utilized in each ONU to serve as upstream transmitter (Tx) transmitting 2.5 Gbit/s on-off keying (OOK) and 10 Gbit/s OFDM traffic, respectively. Moreover, the dynamic bandwidth (and capacity) allocation and fiber-fault protection can also be centralized management by utilizing software-defined networking (SDN) technology in this proposed architecture.

2. Proposed PON Architecture

Fig. 1 shows the proposed 40 Gbit/s TWDM-PON architecture. Here, we use four 2.5 GHz DMLs (λ_1 , λ_2 , λ_3 , and λ_4) to act as downstream wavelengths in the SDN-enabled OLT. Another four WDM wavelengths (λ_5 , λ_6 , λ_7 , and λ_8) are served as the carrier-distributed CW signals to launch into each ONU for upstream traffic, as illustrated in Fig. 1. Besides, the 1×4 array waveguide grating (AWG) and 2×2 optical coupler (OC) are utilized to connect the four downstream and carrier-distributed CW wavelengths for signal traffic. Hence, these wavelengths can transmit

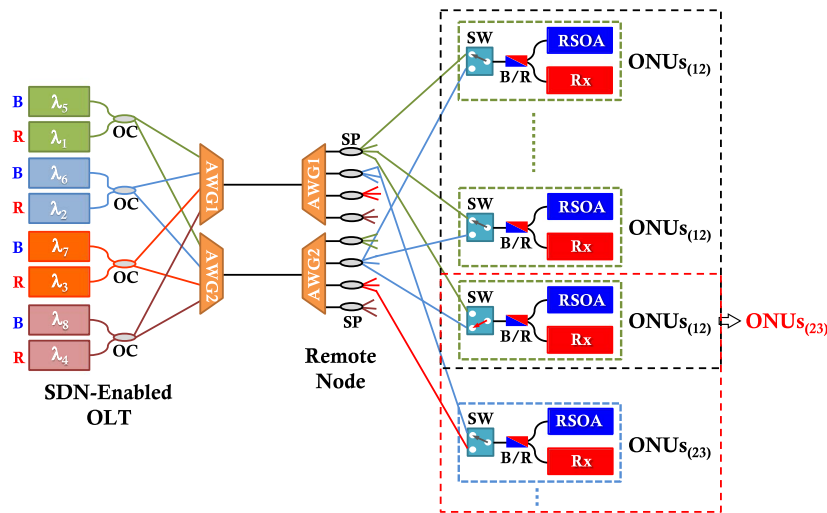


Fig. 2. Proposed 40 Gbit/s downstream TWDM-PON architecture for rearranging ONUs.

through the upper and lower feeder fibers simultaneously and then into each ONU. In the experiment, the wavelengths of λ_1 , λ_2 , λ_3 , and λ_4 and λ_5 , λ_6 , λ_7 , and λ_8 are set at the red- and blue-bands for downstream and upstream transmissions. As we know, the AWG has the spectral periodic property. Thus, λ_1 and λ_5 , λ_2 and λ_6 , λ_3 and λ_7 , and λ_4 and λ_8 can pass through the ports 1, 2, 3, and 4 of AWG, respectively. Moreover, the dynamic bandwidth allocation for end user and active device control for fiber fault protection can be centralized management by utilizing SDN controllers for reliable and flexible PON access network.

The remote node (RN) is consisted of two AWGs and eight $1 \times N$ optical splitters (SPs), as illustrated in Fig. 1. Each ONU is constructed by a 1×2 optical switch (OS), a blue/red-band filter (BRF), a 1.2 GHz RSOA and a 2.5 GHz PIN Rx, as shown in Fig. 1. In addition, the OS of ONU is used to select the transmission path in upper or lower feeder fibers. Here, to achieve the flexible and reliable TWDM-PON access, the whole ONUs are grouped to $ONU_{S(12)}$, $ONU_{S(23)}$, $ONU_{S(34)}$ and $ONU_{S(41)}$, respectively. Hence, the $ONU_{S(12)}$ can be connected to SP_1 and SP_2 of AWG_1 and AWG_2 respectively. Identically, the SP_2 and SP_3 , SP_3 and SP_4 , and SP_4 and SP_1 of AWG_1 and AWG_2 are connected to $ONU_{S(23)}$, $ONU_{S(34)}$ and $ONU_{S(41)}$, respectively, as seen in Fig. 1. Therefore, we set two adjacent downstream signals as a group for capacity allocation. Hence, the downstream wavelengths of λ_1 and λ_2 , λ_2 and λ_3 , λ_3 and λ_4 , and λ_4 and λ_1 are set for four ONU groups.

The SDN-enabled TWDM-PON OLT would define the wavelengths and the TDM time-slots to be the virtual ports, and the OLT's software device drivers could re-map the virtual port-IDs to their corresponding wavelengths and TDM time-slots, then SDN-Controller could install the related flow-table with the virtual port-IDs to manage the traffic flows. The SDN-Controller also would leverage the Openflow Vendor/Experimenter messages, which are the mechanism for proprietary messages within the Openflow protocol, to control OS functions for PON Networks.

In normal status, the OS of each ONU connects to upper feeder fiber for signal traffic. According to the proposed network architecture, the dynamic bandwidth allocation (DBA) for each ONU can be completed by employing SDN technology. Besides, the proposed PON network also can utilize SDN to control the OS of each ONU for selecting the downstream signal for data traffic. As seen in Fig. 2, when the $ONU_{S(12)}$ group require higher capacity for end-user. The 1×2 OS of $ONU_{S(12)}$ can be switched to connect to downstream λ_2 for sharing the capacity of $ONU_{S(23)}$ group via SDN control. Then, the original $ONU_{S(12)}$ could be regarded as $ONU_{S(23)}$ in this PON. That is to say, the four downstream signals could negotiate mutually to arrange the ONU number and DBA operation by SDN-enabled OLT. As a result, the other ONU groups of the proposed PON network also can complete the DBA and capacity allocation.

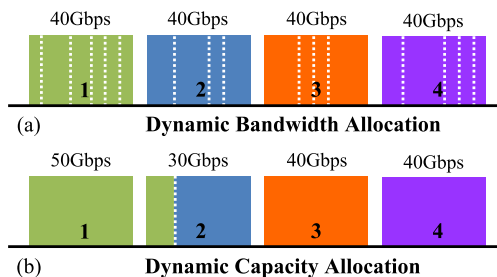


Fig. 3. (a) Schematic diagram for arranging bandwidth allocation dynamically. (b) Dynamic capacity allocation of four ONU groups by using proposed TWDM-PON architecture.

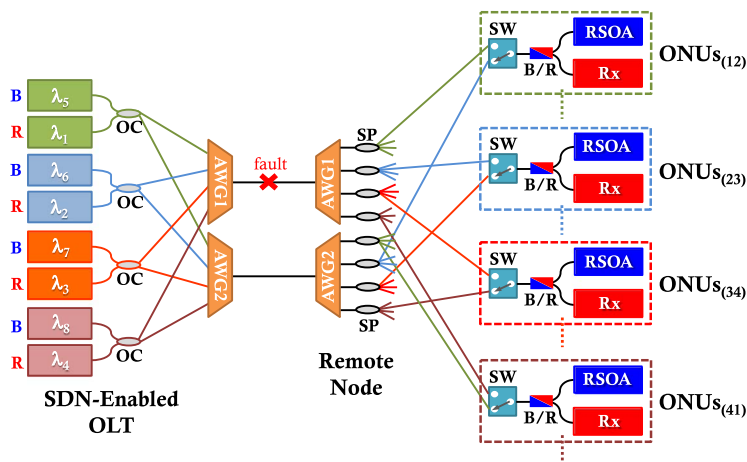


Fig. 4. What happens if a fault occurs in the upper feeder fiber in the proposed TWDM-PON system.

To realize the basic principle of DBA for four ONU groups, Fig. 3(a) shows the schematic diagram for arranging bandwidth allocation dynamically. The bandwidth for each end-user is assigned by SDN-enabled OLT. Moreover, Fig. 3(b) presents the dynamic capacity allocation of four ONU groups by using proposed TWDM-PON architecture. Hence, based on the various bandwidth demand of end-user, we can control DBA mechanism and switch the OS of ONU to achieve capacity allocation for the flexible and reliable data traffic access.

The proposed TWDM-PON architecture also has the advantage of self-protected architecture against fiber fault. According to the PON system, the fiber fault maybe occurs at feeder fiber or distributed fiber due to the vandalism or environment effect. To keep off the fiber fault issue, the proposed self-protected TWDM-PON architecture also can be reached. Initially, the whole OS of ONUs switch to connect to the upper feeder fiber for data transmission. In the proposed PON, if a fault occurs in the upper feeder fiber, as shown in Fig. 4, the whole upstream signals of ONUs would not transmit to SDN-enabled OLT for data link. Therefore, in order to reconnect to the OLT, the OS of each ONU would switch to another point by utilizing medium access control (MAC) layer of ONU, as illustrated in Fig. 4. Then, the whole upstream signals would transmit through the lower feeder fiber for data reconnection. Therefore, each ONU also can decide which switch of OS is connected by itself for signal link, when the downstream is disconnection.

Furthermore, the fiber fault maybe can occur in the distributed fiber (between RN and each ONU). If a fault appears in one of $ONU_{s(23)}$, it will affect the connectivity of OLT and $ONU_{s(23)}$, as shown in Fig. 5. Immediately, the OS of $ONU_{s(23)}$ could also switch to another point for re-connecting data through the another fiber path. In other words, the OS of each ONU could be switched automatically by MAC for connecting the upper or lower feeder fibers for signal transmission. Here, the optical switch (1 dB insertion loss) and tunable filter (3 dB insertion loss) are

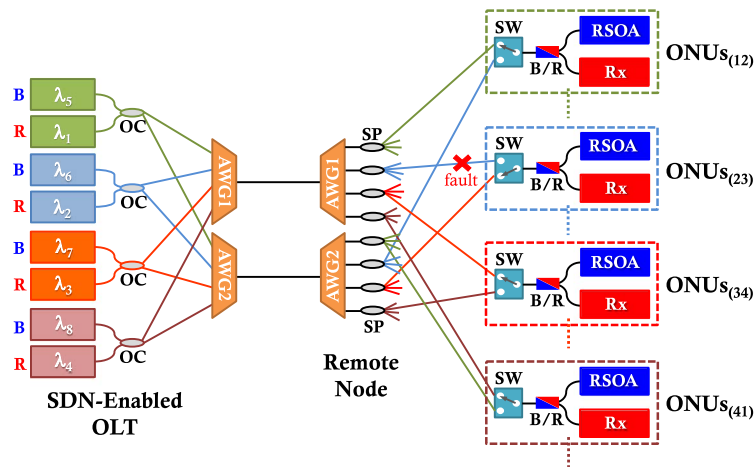


Fig. 5. What happens if a fault occurs in the distribution fiber in the proposed TWDM-PON system.

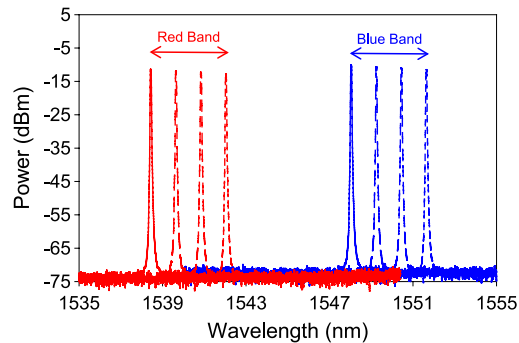


Fig. 6. Output spectra of downstream (blue band) and carrier-distributed CW (red band) wavelengths.

utilized in the measurement. Hence, those two devices would cause 4 dB power budget in the proposed PON system. The switching time of 1×2 optical switch is nearly 7 ms. Hence, the system transfer time would be around 7 ms. As mentioned above, the proposed PON network not only has simple architecture and operation method but has cost-effectiveness as well. As a result, the proposed flexible and reliable PON is very useful for the next-generation access application.

3. Experiment and Discussions

In this section, to verify the signal performance of the proposed flexible and reliable TWDM-PON, an experiment is performed, as illustrated in Fig. 1. In the experiment, the four downstream wavelengths (λ_1 , λ_2 , λ_3 , and λ_4) of 1548.02, 1549.22, 1550.42, and 1551.62 nm and the carrier-distributed CW wavelengths (λ_5 , λ_6 , λ_7 , and λ_8) of 1538.42, 1539.62, 1540.82, and 1542.02 nm are employed in the OLT, respectively. In the measurement, the threshold current and output power of 2.5 GHz DML are 15 mA and 3 dBm, respectively. Fig. 6 presents the output spectra of downstream (blue band) and carrier-distributed CW (red band) wavelengths. The output wavelength is measured by an optical spectrum analyzer (OSA) with a 0.06 nm resolution.

Four 2.5 GHz DMLs employing 16-QAM OFDM modulation are used to achieve 4×10 Gbit/s downstream wavelengths in this experiment. The baseband electrical OFDM signal can be generated by using arbitrary waveform generator (AWG) with Matlab programs. The sampling rate and DAC resolution are set at 5 Gbit/s and 5 bits, and the cyclic prefix (CP) is 1/64. In this measurement, 128 subcarriers of 16-QAM OFDM formats are occupied ~ 2.5 GHz bandwidth

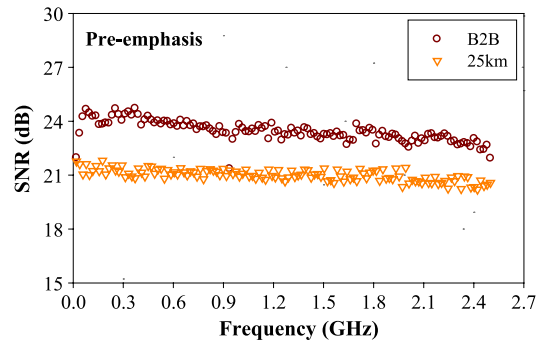


Fig. 7. Measured downstream SNR of each OFDM subcarrier in the frequency bandwidth of 0.0195 to 2.5 GHz at the B2B and a 25 km SMF transmission, respectively.

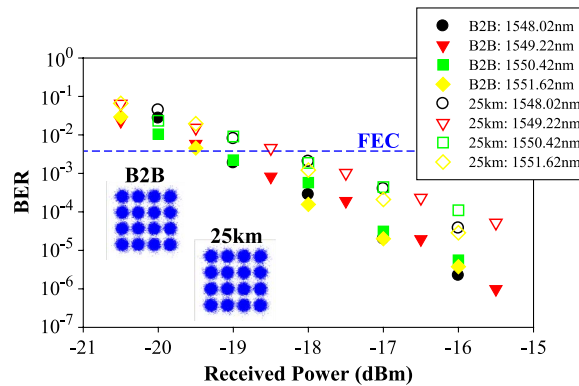


Fig. 8. BER measurements of 10 Gbit/s downstream signal utilizing 16-QAM OFDM modulation with pre-emphasis at the B2B state and a 25 km SMF transmission, respectively.

from 1.95 MHz to 2.50 GHz, with a FFT size of 512 as well. Hence, it can generate a 10 Gbit/s data rate for downstream traffic, and the downstream signal is received by a 2.5 GHz PIN Rx at each ONU. Moreover, the received downstream OFDM signal can be captured by using a real-time sampling oscilloscope for signal demodulation. Here, to achieve the better OFDM signal performance, the pre-emphasis method is also utilized.

Fig. 7 shows the measured downstream signal (1550.42 nm) to noise ratio (SNR) of each OFDM subcarrier in the frequency bandwidth of 0.0195 to 2.5 GHz at the B2B and a 25 km single-mode fiber (SMF) transmission respectively, with pre-emphasis at the received power of -14 dBm. The pre-emphasis can arrange the electrical power of each subcarrier to obtain the better SNR. Therefore, Fig. 7 presents the entire SNRs are larger than 15.6 dB ($BER = 3.8 \times 10^{-3}$) within the bandwidth of 2.5 GHz under the B2B status and a 25 km SMF, respectively.

Here, Fig. 8 shows the bit error rate (BER) measurements of four 10 Gbit/s downstream signals utilizing 16-QAM OFDM modulation with pre-emphasis at the B2B state and a 25 km SMF transmission, respectively. In Fig. 8, the received sensitivities of -19.2 and -18.4 , -19.3 and -18.4 , -19.0 and -18.1 , and -19.4 and -18.6 dBm are observed at the B2B status and a 25 km fiber transmission, respectively, under the forward error correction (FEC) threshold ($BER = 3.8 \times 10^{-3}$). Hence, the measured power penalties of 0.8, 0.9, 0.9 and 0.8 dB are observed in a 25 km SMF transmission at the BER of 3.8×10^{-3} , respectively. The inset of Fig. 8 is the corresponding constellation diagram (λ_3) measuring at the FEC threshold under the B2B status and a 25 km SMF transmission respectively. The observed constellation diagrams are also clear in the B2B and 25 km SMF transmission. As a result, the 4×10 Gbit/s downstream traffic for 25 km fiber link can be finished by employing 16-QAM OFDM modulation via a 2.5 GHz DML. The

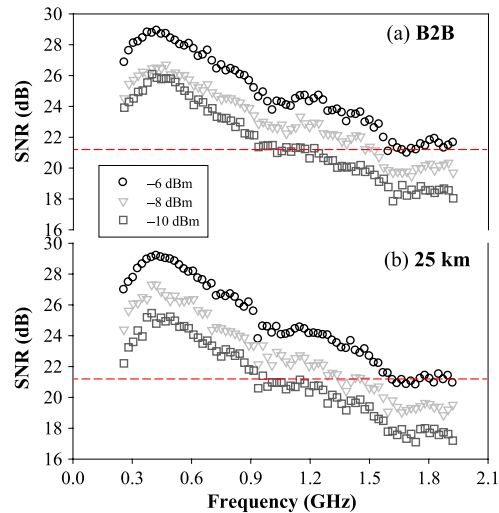


Fig. 9. Measured SNR of each OFDM subcarrier at the B2B state and a 25 km SMF transmission, respectively, while the different CW injection powers of -6 , -8 , and -10 dBm are utilized for launching into RSOA.

four wavelengths in each band (the red band and blue band) are well separated by 1.2 nm; and the downstream and CW seeding signals are produced by temperature controlled lasers. Besides, the 1×4 AWG with crosstalk level of -30 dB can be used, and we believe that the crosstalk from adjacent channel is very small.

In the upstream traffic, we use carrier-distributed CW wavelength from OLT launching into 1.2 GHz RSOA (manufactured by *CIP*) of each ONU for upstream modulation. Here, sampling rate and DAC resolution are 12 GSample/s and 8 -bit by using the AWG. The CP of $1/64$ is used. Besides, 72 subcarriers of 64 -QAM OFDM occupy 1.6642 GHz bandwidth from 0.2578 to 1.922 GHz with a FFT size of 512 . Here, ~ 22 MHz subcarrier spacing and ~ 10 Gbit/s OFDM data rate can be achieved, when electrical 64 -QAM OFDM signal is applied on RSOA directly. Here, the bias current of RSOA is set at 60 mA.

Besides, reusing the downstream signal to generate the upstream signal is also possible and can reduce the number of wavelength used, as shown in [22]–[24]. However, these schemes need to erase the downstream signal for the successful modulation of the upstream, for example, in [22], a residual downstream signal can still be observed after the remodulation using the RSOA. In [23], optimum injection power and bias-current of the FP-LD are required to erase the downstream signal. Hence, in our scheme, we do not directly reuse the downstream signal.

To realize the signal performance of upstream, we first measure the upstream SNR of each OFDM subcarrier in the frequency bandwidth of 0.2578 to 1.922 GHz at the B2B and a 25 km SMF transmission, respectively, under the different launching powers of -6 , -8 and -10 dBm respectively. Fig. 9(a) and (b) present the measured SNR of each OFDM subcarrier at the B2B state and a 25 km SMF transmission, respectively, while the different CW injection powers of -6 , -8 , and -10 dBm are utilized for launching into RSOA. When the injection power is -6 dBm, the entire SNR of each OFDM subcarrier can be achieve FEC limit ($\text{SNR} = 21.2$ dB) at the B2B and 25 km SMF transmission, as illustrated in Fig. 9(a) and (b), respectively. Moreover, as the injection power decreases gradually, the measured SNR in the high frequency subcarrier could not achieve FEC level due to the reduction in relaxation oscillation frequency of the RSOA under the different injected powers. Therefore, when the injected power is -10 dBm, there is a half of OFDM subcarriers cannot achieve FEC limit in both transmission states.

Here, the downstream signal would transmit through 25 km SMF (5 dB loss), an AWG (6 dB loss), a SW (1 dB loss), and a BRG (3 dB loss). These devices need 14 dB power budget. If the downstream signal is 7.5 dBm, then the maximum splitter ratio would be 1×8 (9 dB loss) in the proposed PON access.

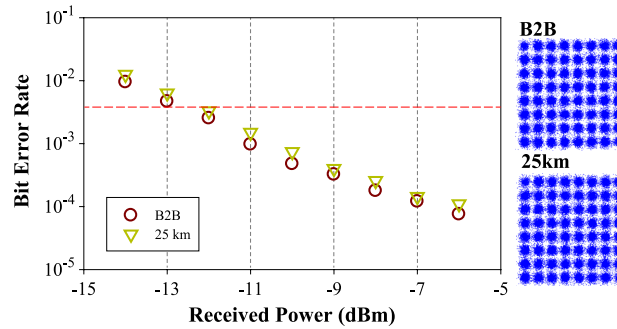


Fig. 10. Upstream BER performances at the B2B and a 25 km SMF transmission, respectively, when an -8 dBm CW signal is launching into RSOA.

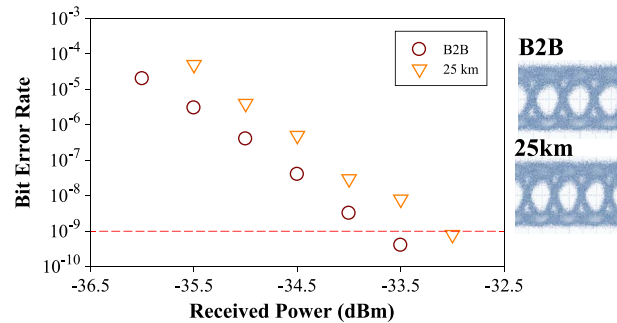


Fig. 11. BER performances of 2.5 Gbit/s NRZ at the B2B status and a 25 km SMF transmission with no dispersion compensation.

As mentioned above, we set the CW injected power at -8 dBm launching into RSOA for the better upstream traffic. Hence, Fig. 10 presents the 10 Gbit/s 64-QAM OFDM upstream BER performances at the B2B and a 25 km SMF transmission, respectively, when an -8 dBm CW signal (1540.82 nm) is launching into RSOA, and the sensitivity powers of -12.5 and -12.1 dBm are also observed at the FEC threshold. Hence, ~ 0.4 dB power penalty is measured after 25 km SMF transmission at the BER of 3.8×10^{-3} .

Then, we will discuss and analyze using OOK modulation for RSOA-based upstream traffic. In this measurement, to achieve the BER of 10^{-9} , the injected power of > -10 dBm must be required. When the injected power of < -10 dBm, the observed BER would be larger than 10^{-9} . Hence, we select the injected CW power at -10 dBm launching into RSOA for 2.5 Gbit/s OOK upstream link. Each RSOA can be modulated at 2.5 Gbit/s non-return to zero (NRZ) format under pseudorandom binary sequence (PRBS) with pattern length of $2^{31} - 1$. The measured upstream signal uses pre-amplification to enhance the BER performance. Fig. 11 displays the BER performances of 2.5 Gbit/s NRZ at the B2B status and a 25 km SMF transmission with no dispersion compensation. The results show that the power penalty of 0.7 dB is obtained. Besides, the corresponding eye diagrams are shown in the right of Fig. 5. The eye diagrams are opened and clear after 25 km fiber transmission. Here, the received sensitivity is -33.0 dBm after 25 km SMF transmission.

According to the measured results of Figs. 10 and 11, the observed sensitivities are -12.1 and -33.0 dBm, respectively, when the RSOA is directly modulated at 10 Gbit/s 64-QAM OFDM and 2.5 Gbit/s OOK formats under an -8 and -10 dBm injection power. Hence, if we want to get more upstream capacity, the received sensitivity must to go down and also reduce the number of ONU. As mentioned above, the downstream signal is generated by direct modulation of a DML, while the upstream signal is generated by the CW light injection into a RSOA. The smaller power penalty of the upstream signal could be due to the reduction of chirp in the optical

injected RSOA. As a result, how to determine the properly modulation format for upstream traffic is a trade-off issue for new generation PON access.

4. Conclusion

In this paper, we proposed and demonstrated a flexible and reliable 40 Gbit/s TWDM-PON access architecture. Here, 4×10 Gbit/s OFDM downstream traffic was achieved by using four 2.5 GHz DMLs in the SDN-enabled OLT. Besides, we also used four CW carrier distributed wavelengths in the OLT for upstream modulation. Here, RSOA was utilized in each ONU to serve as upstream Tx together with 2.5 Gbit/s OOK and 10 Gbit/s OFDM traffic, respectively, under 25 km SMF transmission. Moreover, the dynamic bandwidth (and capacity) allocation and fiber-fault protection also could be achieved by employing new proposed PON architecture and centralized management by utilizing SDN technology.

References

- [1] H. Tamai *et al.*, "First demonstration of coexistence of standard gigabit TDM-PON and code division multiplexed PON architectures toward next generation access network," *J. Lightw. Technol.*, vol. 27, no. 3, pp. 292–298, Feb. 2009.
- [2] C. H. Yeh, C. W. Chow, Y. F. Wu, F. Y. Shih, and S. Chi, "Experimental demonstration of CW light injection effect in upstream traffic TDM-PON," *Opt. Fiber Technol.*, vol. 16, no. 3, pp. 178–181, Jun. 2010.
- [3] "10-gigabit-capable passive optical networks (XG-PON): General requirements," Int. Telecommun. Union, Geneva, Switzerland, G.987.1, 2011.
- [4] P. Vetter, "Next generation optical access technologies," presented at the Eur. Conf. Opt. Commun., Amsterdam, The Netherlands, 2012, Paper Tu.3.G.1.
- [5] W. George, W. Chen, and S. Liu, "Serial 40G submarine deployments," in *Proc. OFC*, 2009, pp. 1–3.
- [6] C. W. Chow, C. H. Yeh, and J. Y. Sung, "OFDM RF power-fading circumvention for long-reach WDM-PON," *Opt. Exp.*, vol. 22, no. 20, pp. 24392–24397, Oct. 2014.
- [7] C. H. Yeh, C. W. Chow, H. Y. Chen, and Y. L. Liu, "115 Gbit/s downstream and 10 Gbit/s upstream TWDM-PON together with 11.25 Gbit/s wireless signal utilizing OFDM-QAM modulation," *Opt. Fiber Technol.*, vol. 20, no. 2, pp. 84–89, Mar. 2014.
- [8] J. Yu, M.-F. Huang, D. Qian, L. Chen, and G.-K. Chang, "Centralized lightwave WDM-PON employing 16-QAM intensity modulated OFDM downstream and OOK modulated upstream signals," *IEEE Photon. Technol. Lett.*, vol. 20, no. 18, pp. 1545–1547, Sep. 2008.
- [9] Y. Luo *et al.*, "Time—and wavelength-division multiplexed passive optical network (TWDM-PON) for next-generation PON stage 2 (NG-PON2)," *J. Lightw. Technol.*, vol. 31, no. 4, pp. 587–593, Feb. 2013.
- [10] C. W. Chow, C. H. Yeh, K. Xu, J. Y. Sung, and H. K. Tsang, "TWDM-PON with signal remodulation and Rayleigh noise circumvention for NG-PON2," *IEEE Photon. J.*, vol. 5, no. 6, Dec. 2013, Art. ID 7902306.
- [11] Z. Li *et al.*, "Experimental demonstration of a symmetric 40-Gb/s TWDM-PON," presented at the Opt. Fiber Commun. Conf., Anaheim, CA, USA, 2013, Paper NTh4F.3.
- [12] Z. Zhou, M. Bi, S. Xiao, Y. Zhang, and W. Hu, "Experimental demonstration of symmetric 100-Gb/s DML-based TWDM-PON system," *IEEE Photon. Technol. Lett.*, vol. 27, no. 5, pp. 470–473, Mar. 2015.
- [13] A. Chowdhury *et al.*, "A survivable protection and restoration scheme using wavelength switching of integrated tunable optical transmitter for high throughput WDM-PON system," presented at the Opt. Fiber Commun. Conf., Los Angeles, CA, USA, 2011, Paper OThK6.
- [14] C. H. Yeh, C. W. Chow, F. Y. Shih, Y. F. Wu, and J. Y. Sung, "Fiber-fault protection WDM-PON using new apparatus in optical networking unit," *Opt. Commun.*, vol. 285, no. 7, pp. 1803–1806, Apr. 2012.
- [15] T. Nishitani, J. Mizuguchi, and H. Mukai, "Experimental study of Type B protection for a TWDM-PON system," *J. Opt. Commun. Netw.*, vol. 7, no. 3, pp. A414–A420, Mar. 2015.
- [16] C. H. Yeh *et al.*, "Ring-based WDM access network providing both Rayleigh backscattering noise mitigation and fiber-fault protection," *J. Lightw. Technol.*, vol. 30, no. 20, pp. 3211–3218, Oct. 2012.
- [17] C. W. Chow, C. H. Yeh, J. Y. Sung, and C. W. Hsu, "Wired and wireless convergent extended-reach optical access network using direct-detection of all-optical OFDM super-channel signal," *Opt. Exp.*, vol. 22, no. 25, pp. 30719–30724, Dec. 2014.
- [18] Y.-C. Chi, P.-C. Peng, H.-H. Lu, and G.-R. Lin, "Coherently injection-locked weak-resonant-cavity laser diode for optical 16-QAM-OFDM transmission at 4 Gb/s," in *Proc. IEEE WOCC*, 2012, pp. 138–139.
- [19] M. Jarschel, T. Zinner, T. Hossfeld, P. Tran-Gia, and W. Kellerer, "Interfaces, attributes, and use cases: A compass for SDN," *IEEE Commun. Mag.*, vol. 52, no. 6, pp. 210–217, Jun. 2014.
- [20] M. Forzati and A. Gavler, "Flexible next-generation optical access," in *Proc. IEEE ICTON*, 2013, pp. 1–8.
- [21] N. Cvijetic *et al.*, "SDN and OpenFlow for dynamic flex-grid optical access and aggregation networks," *J. Lightw. Technol.*, vol. 32, no. 4, pp. 864–870, Feb. 2014.
- [22] B. W. Kim, "RSOA-based wavelength-reuse gigabit WDM-PON," *J. Opt. Soc. Korea*, vol. 12, pp. 337–345, 2008.
- [23] Y.-C. Su, Y.-C. Chi, H.-Y. Chen, and G.-R. Lin, "Data erasing and rewriting capabilities of a colorless FPLD based carrier-reusing transmitter," *IEEE Photon. J.*, vol. 7, no. 3, Jun. 2015, Art. ID 7201212.
- [24] C.-T. Tsai, Y.-C. Chi, and G.-R. Lin, "Power fading mitigation of 40-Gbit/s 256-QAM OFDM carried by colorless laser diode under injection-locking," *Opt. Exp.*, vol. 23, no. 22, pp. 29065–29078, Nov. 2015.